

Simple security proof of coherent-one-way quantum key distribution

Rui-Qi Gao,¹ Yuan-Mei Xie,¹ Jie Gu,¹ Wen-Bo Liu,¹ Chen-Xun Weng,¹ Bing-Hong Li,¹ Hua-Lei Yin,^{1,*} and Zeng-Bing Chen^{1,†}

¹*National Laboratory of Solid State Microstructures,
School of Physics and Collaborative Innovation Center of Advanced
Microstructures, Nanjing University, Nanjing 210093, China*
(Dated: August 11, 2021)

Coherent-one-way quantum key distribution (COW-QKD), possessing the simple experimental setup and the ability against the photon-number-splitting attack, has been implemented in various experiments and commercial applications. However, recent works have proved that current COW-QKD with key rate scaling linearly with transmittance is totally insecure under the zero-error attack. This conclusion leads to a crucial consequence that all the current attempts for practicalization are in vain. To solve this pending issue, here we conduct a minor revision on original COW-QKD while maintaining the original experimental setup as well as the simplicity of implementation. By more precisely estimating the amount of leaked information, we provide an explicit unconditional secure key rate which scales with 0.7% of the bound that quadratically scales with transmittance. Our work provides a revised COW-QKD which guarantees the availability of the current implementations of COW-QKD within 100 km and establishes the theoretical foundations for further application.

I. INTRODUCTION

Quantum key distribution (QKD) [1, 2], whose security is guaranteed by quantum laws, allows secret key distribution between two distant parties. Since the Bennett-Brassard 1984 (BB84) protocol [1] was first proposed, numerous QKD schemes have been rapidly developed [3–5]. To defeat detector attacks [4, 6], one viable approach is the measurement-device-independent QKD [7, 8] which has been implemented at long distance [9, 10]. Recently, twin-field QKD [11–19] can also solve this issue and significantly improve the secret key rate. Another strong restriction in practical QKD is the photon-number-splitting attack [20] in the source side. For example, the coherent-state-based (non-random phase) BB84 protocol can only realize the secure key transmission over 15 km. To overcome this obstacle, several main approaches such as decoy-state methods [21–23], strong reference-pulse methods [24], non-orthogonal coding methods [25–27] and distributed-phase-reference methods [28–31] have been proposed.

As a type of distributed-phase-reference protocol, the coherent-one-way (COW) QKD [30] receives considerable attention because of its simple and convenient experimental implementation [32–39], which has been deployed in practical quantum communication networks [40, 41]. Considering *the restricted type of collective attacks* [42], the key rate depends linearly on transmittance η . Besides, *a variant of the COW-QKD* with a security proof against general attacks has also been proposed in 2012 [43], and the resulting key rate “appears to” be of order $O(\eta^2)$. Recently, a novel security proof using semidefinite programming techniques [44] shows that the

transmission distance of COW-QKD with active-basis choice is only 20 kilometers. So far, all COW-QKD experiments [34, 36–39], including the long-distance experiment [35, 45], still employ the original security proof [42], in which the key rate is of order $O(\eta)$. These experimental results show the great practicability and potential of the COW-QKD. Nevertheless, the unconditional security proof of COW-QKD is still a long-standing open question.

Even worse, the so called “zero-error attack” [46, 47] can eavesdrop without breaking the coherence between adjacent non-vacuum pulses (no bit error). Consequently, the original COW-QKD (simply COW-QKD hereafter) is totally insecure if the key rate scales as $O(\eta)$; rather, the given attack restricts the secure key rate scaling a little higher than η^2 [46, 47]. As the zero-error attack severely threatens the commercialization of the COW-QKD, a security proof, if possible at all, becomes a more urgent task.

In this work, we adopt a subtle modification on COW-QKD and propose a security proof with a precise phase error rate estimation. The modification keeps all the experiment equipment unchanged and maintains the easiness of implementation. With detailed observations on the monitoring line, we estimate the upper bound on the phase error rate instead of only checking the coherence between adjacent non-vacuum states. We present the secure lower bound of the key rate that is almost equal to $0.007\eta^2$, which is much lower than the upper bound ($\sim \eta^2$) derived in [46, 47]. It is worth mentioning that, our secure lower bound of the key rate is almost 10 times higher than the key rate given by the variant of the COW-QKD in Ref. [43], considering that we effectively evaluate the impact of vacuum states and give the analytical expression.

*Electronic address: hlyin@nju.edu.cn

†Electronic address: zbchen@nju.edu.cn

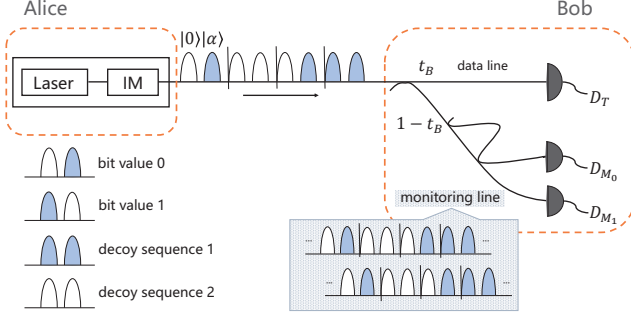


FIG. 1: Schematic of the revised COW-QKD. Alice randomly sends the sequence of states $|0\rangle_{2k-1}|\alpha\rangle_{2k}$, $|\alpha\rangle_{2k-1}|0\rangle_{2k}$, $|\alpha\rangle_{2k-1}|\alpha\rangle_{2k}$ and $|0\rangle_{2k-1}|0\rangle_{2k}$ to Bob. Then, a beam-splitter of transmittance t_B distributes incoming pulses into the data line and the monitoring line at the receiving side, Bob. The quantum states can be experimentally realized through Alice modulating $|0\rangle$ or $|\alpha\rangle$ using intensity modulator (IM) at each time bin. Compared with the original COW-QKD where the sequences of states can be prepared in the similar way, there is no any extra technical requirement in our modification. D_T , D_{M_0} and D_{M_1} are the single-photon detectors.

II. REVIEW OF COW-QKD

In original COW-QKD, the sender, Alice, encodes the logic bit 0 and 1 into a pair of coherent states (non-random phase) $|0_k\rangle = |0\rangle_{2k-1}|\alpha\rangle_{2k}$ and $|1_k\rangle = |\alpha\rangle_{2k-1}|0\rangle_{2k}$ at two time points $2k-1$ and $2k$ ($k = 1, 2, \dots, K$), where $|0\rangle$ is a vacuum state and $|\alpha\rangle$ is a coherent state with mean photon-number $\mu = |\alpha|^2$. Besides, Alice also sends a two-pulse sequence $|\alpha\rangle_{2k-1}|\alpha\rangle_{2k}$ which is defined as a decoy sequence. Since all non-vacuum pulses share a common phase, Alice can use a mode-locked continuous wave laser followed by an intensity modulator to prepare weak coherent pulses.

Then the pulses are transmitted to the receiver, Bob, through a quantum channel characterized by η . Bob employs an asymmetric beam-splitter with the transmission coefficient t_B (passive-basis choice measurement) to split the incoming pulses into the data line and the monitoring line. We note that Bob can also use an optical switch (active-basis choice measurement) to replace the beam-splitter. On the data line, Bob obtains the raw key by measuring the arrival time of each pair of pulses with the detector D_T . On the monitoring line, Bob checks the coherence between adjacent non-vacuum pulses by observing the measurement outcome of a Mach-Zehnder interferometer with two detectors D_{M_0} and D_{M_1} . The information leakage can be detected by the broken coherence, which can be reflected by the visibility $V = [P(D_{M_0}) - P(D_{M_1})]/[P(D_{M_0}) + P(D_{M_1})]$, where $P(D_{M_0})$ [$P(D_{M_1})$] is the probability that the detector D_{M_0} (D_{M_1}) clicks. Alice and Bob also take a random subset of data on the data line to test the bit error rate E_b . The security proof and the secure key rate of

the COW-QKD are given based on these two parameters, E_b and V [42].

Nevertheless, recent studies have introduced the so-called zero-error attack [46, 47]. On the one hand, since the signals sent by Alice are linearly independent, Eve can adopt an unambiguous state discrimination measurement to distinguish each signal sent by Alice without introducing error on the data line. On the other hand, the vacuum state in signals naturally breaks the coherence between adjacent pulses. Taking advantage of this property, Eve can resend Bob blocked signal sequences which preserve the coherence among consecutive nonempty pulses. Thus, all the security proofs of the COW-QKD, which rely on analyzing the coherence, appear to be unreliable.

III. MODIFICATION OF COW-QKD

In our work, as shown in Fig. 1, we slightly modify the original COW protocol, where only some operational and computational modification are adopted. In the revised COW-QKD, Alice sends four kinds of two-pulse sequences $|0_k\rangle = |0\rangle_{2k-1}|\alpha\rangle_{2k}$, $|1_k\rangle = |\alpha\rangle_{2k-1}|0\rangle_{2k}$, $|\alpha\rangle_{2k-1}|\alpha\rangle_{2k}$ and $|0\rangle_{2k-1}|0\rangle_{2k}$. Here $|0_k\rangle$ and $|1_k\rangle$ are encoded as in the original COW-QKD, and $|\alpha\rangle_{2k-1}|\alpha\rangle_{2k}$ and $|0\rangle_{2k-1}|0\rangle_{2k}$ are decoy sequences. When evaluating the secure key rate, Alice no longer estimates the visibility V to quantify the leaked information. Instead, she calculates the more finely sorted gains $Q_{0\alpha}^{M_i}$, $Q_{\alpha 0}^{M_i}$, $Q_{\alpha\alpha}^{M_i}$ and $Q_{00}^{M_i}$ ($i = 0$ or 1) to estimate the phase error rate, where the superscript M_i represents the clicking detector D_{M_i} on the monitoring line announced by Bob, the subscript refers to the corresponding sequence $|0\rangle_{2k-1}|\alpha\rangle_{2k}$, $|\alpha\rangle_{2k-1}|0\rangle_{2k}$, $|\alpha\rangle_{2k-1}|\alpha\rangle_{2k}$ and $|0\rangle_{2k-1}|0\rangle_{2k}$ sent by Alice, respectively. Here, we need to clarify that, if multiple detectors click corresponding to every pair of states, Bob regards this event as one of these detectors clicking, randomly [48, 49]. The other operations are the same as those in the original COW-QKD. As the experimental setup remains unchanged, the revised COW protocol is still implementable, at the same time, which is immune to collective attacks.

IV. SECURITY PROOF

In order to provide the security proof of the revised COW-QKD, we introduce a virtual entanglement-based protocol as follows. Here we redefine k -th optical modes $|0_z\rangle = |0\rangle_{2k-1}|\alpha\rangle_{2k}$ and $|1_z\rangle = |\alpha\rangle_{2k-1}|0\rangle_{2k}$, where we omit the label k for simplicity of presentation. Let $|0_x\rangle = (|0_z\rangle + |1_z\rangle)/\sqrt{N^+}$ and $|1_x\rangle = (|0_z\rangle - |1_z\rangle)/\sqrt{N^-}$, where $N^\pm = 2(1 \pm e^{-\mu})$ are the normalization factors, be two non-classical optical modes. We introduce an ancillary qubit, with $|\pm z\rangle$ and $|\pm x\rangle$ being the eigenstates of qubit's Pauli operators Z and X , respectively. Alice prepares K

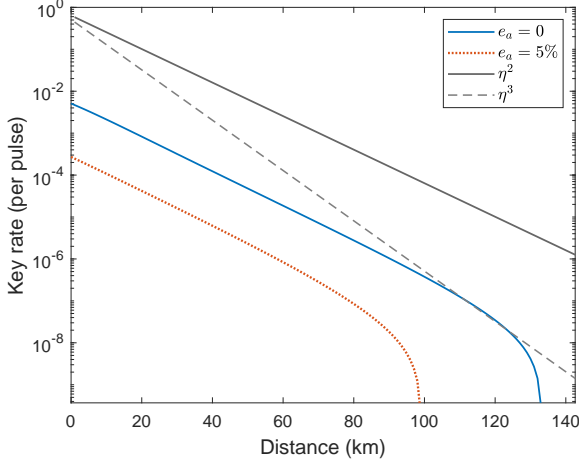


FIG. 2: Secret key rates in the asymptotic case using passive-basis choice with different misalignment errors, $e_a = 0$ and 5%. The key rate scales linearly with $0.007\eta^2$ when $e_a = 0$, which is much lower than the upper bound on secret key rate of order $O(\eta^2)$ given in Refs. [46, 47].

pairs of entangled state

$$\begin{aligned} |\psi\rangle &= \frac{1}{\sqrt{2}}(|+\rangle_A |0_z\rangle_{A'} + |-\rangle_A |1_z\rangle_{A'}) \\ &= \frac{\sqrt{N^+}}{2} |+\rangle_A |0_x\rangle_{A'} + \frac{\sqrt{N^-}}{2} |-\rangle_A |1_x\rangle_{A'}, \end{aligned} \quad (1)$$

where the subscript A denotes the ancillary qubit kept by Alice and A' represents the optical mode sent to Bob. Alice randomly measures the ancillary qubit in the Z or X basis and then acquires the raw keys $\tilde{\mathbf{Z}}_A$ from the Z basis and $\tilde{\mathbf{X}}_A$ from the X basis, respectively. Then, she sends optical modes to Bob through insecure quantum channel. Same as the practical revised COW protocol, the optical modes are detected randomly on the data line or monitoring line. When observing the detector D_T clicks at the previous moment \mathcal{T}_0 (the latter moment \mathcal{T}_1), Bob records the bit values 0 (1) as the raw key in $\tilde{\mathbf{Z}}_B$. Besides, the raw key $\tilde{\mathbf{X}}_B$ are obtained by Bob observing on the monitoring line. Detector D_{M_0} (D_{M_1}) clicking denotes bit value 0 (1).

Let $H_{\min}^\epsilon(\tilde{\mathbf{Z}}_A|E)$ be the smooth min-entropy characterizing the average probability that Eve guesses $\tilde{\mathbf{Z}}_A$ correctly using her optimal strategy with access to the correlations stored in her quantum memory [50]. Let $H_{\max}^\epsilon(\tilde{\mathbf{Z}}_A|\tilde{\mathbf{Z}}_B)$ be the smooth max-entropy corresponding to the number of extra bits needed to reconstruct the value of $\tilde{\mathbf{Z}}_A$ using $\tilde{\mathbf{Z}}_B$ up to a failure probability of ϵ [51]. For latter use, let us denote the binary Shannon entropy as $h(a) = -a \log_2 a - (1-a) \log_2 (1-a)$ and the size of $\tilde{\mathbf{Z}}_A$ as n_z . $\tilde{\mathbf{X}}'_A$ is the bit string Alice would have obtained if she had measured in the X basis, which is measured in the Z basis actually. Therefore, we have the

smooth max-entropy $H_{\max}^\epsilon(\tilde{\mathbf{X}}'_A|B) \leq n_z h(E_x)$ in the asymptotic limit, where E_x is the bit error rate in the X basis. By exploiting the method of uncertainty relation for smooth entropies [52], the asymptotic secure key rate of the virtual entanglement-based protocol can be given by

$$\begin{aligned} \tilde{R} &= \frac{1}{\mathcal{P}_z K} [H_{\min}^\epsilon(\tilde{\mathbf{Z}}_A|E) - H_{\max}^\epsilon(\tilde{\mathbf{Z}}_A|\tilde{\mathbf{Z}}_B)] \\ &= \frac{1}{\mathcal{P}_z K} [n_z - H_{\max}^\epsilon(\tilde{\mathbf{X}}'_A|B) - n_z f h(E_z)] \\ &= Q_z [1 - h(E_x) - f h(E_z)], \end{aligned} \quad (2)$$

where $Q_z = n_z/(\mathcal{P}_z K) = (Q_{0_z}^{\mathcal{T}_0} + Q_{0_z}^{\mathcal{T}_1} + Q_{1_z}^{\mathcal{T}_0} + Q_{1_z}^{\mathcal{T}_1})/2$ is the gain that Alice measures in the Z basis and Bob detects on the data line, \mathcal{P}_z is the probability that Alice measures in the Z basis and Bob measures on the data line. Here f denotes the efficiency of error correction; E_z is the bit error rate in the Z basis. Moreover, we emphasize that when using the entropic uncertainty relation the signals detected by Bob's device should be independent of the basis choices by Alice and Bob [53]. This requirement can naturally be satisfied when measuring with active-basis choice [43, 44], but it needs to be cautiously considered when applying the passive-basis choice measurement. Under the passive-basis choice measurement, Eve can apply classical wavelength attacks [54] to partly control Bob's basis selection and cause the weak basis-choice flaws. Nevertheless, the secure key rate only slightly decreases when one carefully characterizes wavelength to minimize this effect [55, 56]. Recently, the passive-basis choice measurement is still widely utilized in various QKD protocols [57–63]. In this work, under the passive-basis choice measurement, we assume that the beam-splitter is not controlled by the eavesdropper and use the squashing model [48, 49] at the measurement setup.

In fact, the virtual entanglement-based protocol can be converted to an equivalent prepare-and-measure non-classical protocol, i.e., Alice directly prepares optical modes rather than preparing entangled states and measuring the ancillary qubit system. When Alice chooses the Z basis, she directly sends optical modes $|0_z\rangle$ and $|1_z\rangle$ each with probability $1/2$. If Alice selects the X basis, she directly sends non-classical optical modes $|0_x\rangle$ and $|1_x\rangle$ with probability $N^+/4$ and $N^-/4$, respectively. The above facts can be directly seen from the density matrices of the Z basis and the X basis, which are equal in the non-classical protocol, i.e.,

$$\begin{aligned} \rho &= (|0_z\rangle\langle 0_z| + |1_z\rangle\langle 1_z|)/2 \\ &= (N^+ |0_x\rangle\langle 0_x| + N^- |1_x\rangle\langle 1_x|)/4. \end{aligned} \quad (3)$$

Therefore, the bit error rate E_z can be directly obtained by the observed gain,

$$E_z = \frac{Q_{0_z}^{\mathcal{T}_1} + Q_{1_z}^{\mathcal{T}_0}}{Q_{0_z}^{\mathcal{T}_0} + Q_{0_z}^{\mathcal{T}_1} + Q_{1_z}^{\mathcal{T}_0} + Q_{1_z}^{\mathcal{T}_1}}, \quad (4)$$

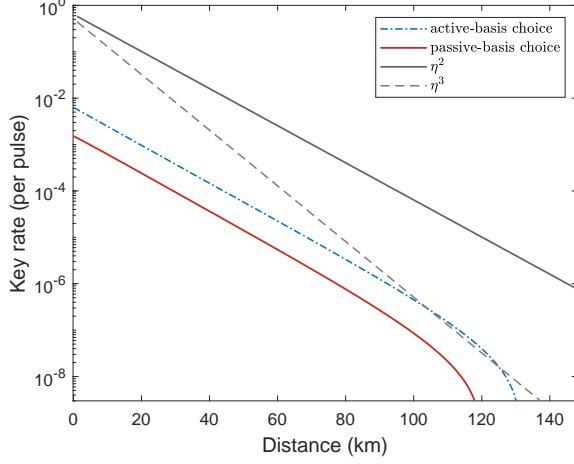


FIG. 3: Comparison of secret key rates under passive-basis choice measurement and active-basis choice measurement in the asymptotic case. The misalignment error e_a is set to be 2%.

where $Q_{w_z}^{\mathcal{T}_j}$ represents Alice sending optical mode $|w_z\rangle$ ($w = 0$ or 1) and Bob having a click at \mathcal{T}_j ($j = 0$ or 1) moment on the data line, and we have $Q_z = (Q_{0_z}^{\mathcal{T}_0} + Q_{0_z}^{\mathcal{T}_1} + Q_{1_z}^{\mathcal{T}_0} + Q_{1_z}^{\mathcal{T}_1})/2$. Similarly, the bit error rate of the X basis can be given by

$$E_x = \frac{N^+ Q_{0_x}^{M_1} + N^- Q_{1_x}^{M_0}}{N^+ (Q_{0_x}^{M_0} + Q_{0_x}^{M_1}) + N^- (Q_{1_x}^{M_0} + Q_{1_x}^{M_1})} \quad (5)$$

$$= \frac{N^+ Q_{0_x}^{M_1} + [2(Q_{0_z}^{M_0} + Q_{1_z}^{M_0}) - N^+ Q_{0_x}^{M_0}]}{2(Q_{0_z}^{M_0} + Q_{0_z}^{M_1} + Q_{1_z}^{M_0} + Q_{1_z}^{M_1})},$$

where $Q_{w_{x(z)}}^{M_i}$ represents Alice sending optical mode $|w_{x(z)}\rangle$ and Bob having a click with detector D_{M_i} on the monitoring line. In the second equation we use the relation $N^+ Q_{0_x}^{M_i} + N^- Q_{1_x}^{M_i} = 2(Q_{0_z}^{M_i} + Q_{1_z}^{M_i})$, which is acquired by Eq. (3).

Let us go back to the practical revised COW-QKD protocol. Note that if Alice directly prepares the encoding sequence $|0\rangle_{2k-1} |\alpha\rangle_{2k}$ or $|\alpha\rangle_{2k-1} |0\rangle_{2k}$ with equal probability, the eavesdropper Eve cannot distinguish this step from the following virtual step: Alice prepares an entangled state $|\psi\rangle$ and measures the ancillary qubit in the Z basis. Consequently, Alice's raw key in revised COW-QKD is the same with \mathbf{Z}_A . The secret key rate of the revised COW-QKD protocol in the asymptotic limit can be written as

$$R = Q [1 - h(E_p^u) - f h(E_b)], \quad (6)$$

where $Q = Q_z$ and $E_b = E_z$ are the gain and bit error rate. The phase error rate E_p^u is upper bound on the average error probability [64] that Bob guesses Alice's bit string \mathbf{X}'_A in the virtual entanglement-based protocol. In

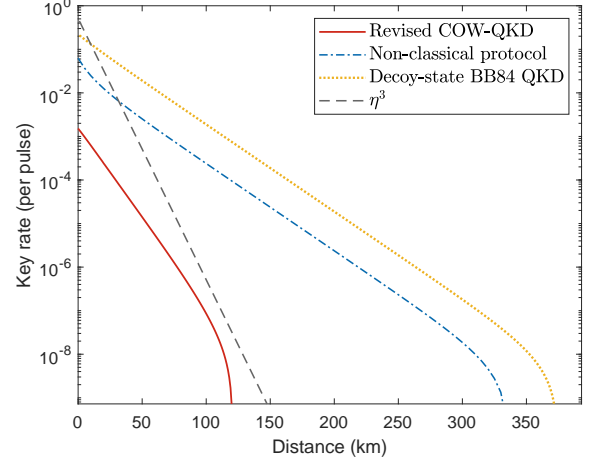


FIG. 4: Comparison of asymptotic secret key rates of the revised COW-QKD, our non-classical protocol and the decoy-state BB84 QKD. The misalignment error $e_a = 2\%$ is set to be the same. The non-classical protocol in our work can reach the key rate of order $O(\eta)$.

practice, Alice does not measure those qubits in the X basis, which means that one cannot directly acquire the gains $Q_{0_x}^{M_0}$ and $Q_{0_x}^{M_1}$. However, we can exploit the gains of other quantum states $|\alpha\rangle_{2k-1} |\alpha\rangle_{2k}$ and $|0\rangle_{2k-1} |0\rangle_{2k}$ to estimate the upper bound $\overline{Q}_{0_x}^{M_1}$ and the lower bound $\underline{Q}_{0_x}^{M_0}$. The phase error rate E_p^u of the revised COW-QKD protocol can be given by

$$E_p^u = \frac{N^+ \overline{Q}_{0_x}^{M_1} + [2(Q_{0_z}^{M_0} + Q_{1_z}^{M_0}) - N^+ \underline{Q}_{0_x}^{M_0}]}{2(Q_{0_z}^{M_0} + Q_{0_z}^{M_1} + Q_{1_z}^{M_0} + Q_{1_z}^{M_1})}, \quad (7)$$

where we use the relation of gain between the non-classical protocol and the revised COW-QKD protocol, i.e., $Q_{0_z}^{M_i} = Q_{0_x}^{M_i}$ and $Q_{1_z}^{M_i} = Q_{1_x}^{M_i}$. Under collective attacks, we have the upper bound $\overline{Q}_{0_x}^{M_1}$ and the lower bound $\underline{Q}_{0_x}^{M_0}$ by using the method of Refs. [16, 65]. Details can be found in Appendix A. We remark that the security of the revised COW-QKD protocol can be extended against coherent attacks by using Azuma's inequality [66].

V. SIMULATION

In our simulation, we assume the dark-count rate $p_d = 10^{-9}$ and the detection efficiency $\eta_d = 99\%$. The correction efficiency f is set as 1.1. The linear lossy channel is characterized by a transmittance $\eta = 10^{-0.02L}$. The transmission coefficient t_B of the asymmetric beam splitter is given by the optimization algorithm.

We present the secret key rate of the revised COW-QKD using a passive-basis choice measurement with different misalignment errors in Fig. 2. Compared with η^2

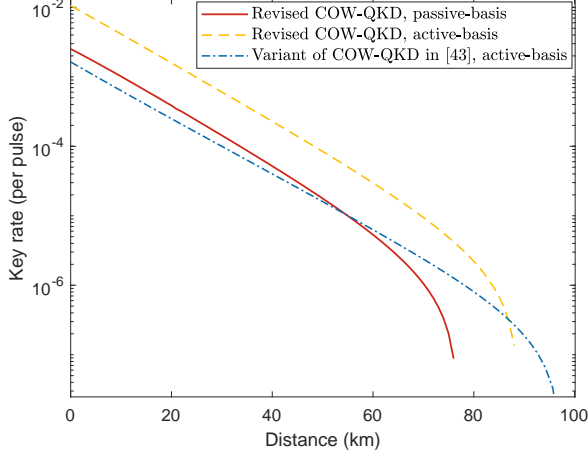


FIG. 5: Comparison of asymptotic secret key rates of revised COW-QKD in this work and a variant of COW-QKD under active-basis choice measurement [43]. The misalignment error e_a is set as 1% and the dark count rate is set as 10^{-7} . The variant of COW-QKD uses 6 optical pulses in each signal block and all blocks of signals share a common phase. Our work under passive-basis choice measurement can still surpass the variant of COW-QKD using active-basis choice measurement within 50 km.

and η^3 , the lower bound on the key rate scales at most $0.007\eta^2$ and is much lower than the upper bound on the key rate given in [46, 47]. The key rate of the revised COW-QKD is barely close to η^3 even if the misalignment error $e_a = 0$. The secret key rate under an active-basis choice measurement on the receiving side is also considered. The numerical results of secret key rates under passive-basis choice measurement and active-basis choice measurement are presented in Fig. 3. Here we also calculate the key rate of the non-classical protocol under passive-basis choice measurement. Comparing the result of the non-classical protocol with the decoy-state BB84 protocol [22, 23] in Fig. 4, we can find that the non-classical protocol also achieves a key rate of order $O(\eta)$.

Additionally, we compare the revised COW-QKD in this work with the variant of COW-QKD [43] in Fig. 5. The variant of COW-QKD is considered in the case where all different 3-signal blocks (including 6 optical pulses) share the same phase and Bob applies the active-basis choice measurement setup. In Fig. 5, the dark-count rate p_d is set as 10^{-7} . The result reveals that the lower bound on the key rate for revised COW-QKD under passive-basis choice and active-basis choice measurement are both tighter than the result given by the variant of COW-QKD.

VI. CONCLUSION

In this work, with a reliable and complete security analysis, the revised COW-QKD is secure under general

attacks. The security proof no longer relies on the coherence between adjacent pulses to detect eavesdropping. Instead, we more finely sort the observed quantities to estimate the upper bound on the phase error rate and calculate the lower bound on secure key rate of the revised COW-QKD. Our result is much lower than the upper bound on key rate derived in recent studies [46, 47], but tighter than the lower bound on the key rate of the variant COW-QKD [43] because we utilize the vacuum states more effectively. With our delicate modification, all current experiment setups continue to be useful and our work paves the way for the secure implementation of revised COW-QKD.

Acknowledgments

We thank Charles Ci Wen Lim, Nicolas Gisin and Ignatius William Primaatmaja for enlightening discussion and making the security proof of this work more rigorous. We gratefully acknowledge support from the National Natural Science Foundation of China (under Grant No. 61801420); the Key-Area Research and Development Program of Guangdong Province (under Grant No. 2020B0303040001); the Fundamental Research Funds for the Central Universities (under Grant No. 020414380182). R.-Q.G. and Y.-M.X. contributed equally to this work.

Appendix A: Upper bound on phase error rate

Here, we first consider the case that Bob applies a passive-basis choice to distribute incoming pulses into the data line and the monitoring line. The gain of the state $|\phi\rangle$ heralded by the detector D_{M_i} ($i = 0$ or 1) clicking can be given by

$$Q_{\phi}^{M_i} = \langle \phi | \hat{\mathcal{M}}_i^+ \hat{\mathcal{M}}_i | \phi \rangle, \quad (\text{A1})$$

where $\hat{\mathcal{M}}_i$ is the Kraus operator corresponding to the announcement of the detector D_{M_i} .

In the non-classical protocol, the gains of the states $|0_z\rangle$ and $|1_z\rangle$ detected by detector D_{M_i} on the monitoring line, i.e., $Q_{0_z}^{M_i}$ and $Q_{1_z}^{M_i}$, can be written as $Q_{0_z}^{M_i} = Q_{1_z}^{M_i} = (1 - p_d)^2 e^{-t_B \mu \eta} c_1 (1 - c_1)$, where $c_1 = (1 - p_d) e^{-(1-t_B)\mu\eta/2}$. The gains $Q_{0_x}^{M_1}$ and $Q_{0_x}^{M_0}$ of the non-classical states $|0_x\rangle$ on the monitoring line are $Q_{0_x}^{M_0} = \frac{2}{N^+} (1 - p_d)^3 (1 - c_1) [e^{-(1+t_B)\mu/2} c_2 + e^{-(1-t_B)\mu\eta/2} c_3]$ and $Q_{0_x}^{M_1} = \frac{2}{N^+} (1 - p_d)^2 c_1 \{ e^{-(1+t_B)\mu/2} [c_4 - (1 - p_d) c_2] + c_3 (1 - c_1) \}$, where the parameters $c_2 = e^{(1-t_B)\mu(1-\eta)/2} + e^{-(1-t_B)\mu(1-\eta)/2}$, $c_3 = e^{-t_B \mu \eta} - e^{-t_B \mu}$ and $c_4 = e^{(1-t_B)\mu/2} + e^{-(1-t_B)\mu/2}$.

In the revised COW-QKD protocol, since the non-classical state $|0_x\rangle$ cannot be acquired, we cannot directly estimate the gain $Q_{0_x}^{M_i} = \langle 0_x | \hat{\mathcal{M}}_i^+ \hat{\mathcal{M}}_i | 0_x \rangle$. We express

$|0_x\rangle$ using states $|0,0\rangle$, $|\alpha,\alpha\rangle$ and $|\beta,\beta\rangle$ as follows.

$$|0_x\rangle = \frac{e^{-\mu}|0,0\rangle + |\alpha,\alpha\rangle - (1 - e^{-\mu})|\beta,\beta\rangle}{e^{-\mu/2}\sqrt{2(1 + e^{-\mu})}}, \quad (\text{A2})$$

where the state $|\beta\rangle = (|\alpha\rangle - e^{-\mu/2}|0\rangle)/\sqrt{1 - e^{-\mu}}$ is the normalized non-vacuum part of the state $|\alpha\rangle$. The pairs of states $|0,0\rangle$ and $|\alpha,\alpha\rangle$ correspond to the decoy sequences sent by Alice. In this way, we can rewrite the gain $Q_{0x}^{M_i}$ as

$$\langle 0_x | \hat{\mathcal{M}}_i^+ \hat{\mathcal{M}}_i | 0_x \rangle = \sum_{l,k} s_l s_k \langle \phi_l | \mathcal{M}_i^+ \mathcal{M}_i | \phi_k \rangle, \quad (\text{A3})$$

where $|\phi_l\rangle, |\phi_k\rangle \in \{|0,0\rangle, |\alpha,\alpha\rangle, |\beta,\beta\rangle\}$, s_l and s_k are the corresponding coefficients of the state in Eq. (A2). By utilizing the Cauchy inequality [16, 65], we have

$$|s_l s_k \langle \phi_l | \mathcal{M}_i^+ \mathcal{M}_i | \phi_k \rangle| \leq |s_l s_k| \sqrt{|\hat{\mathcal{M}}_i | \phi_l \rangle|^2} \sqrt{|\hat{\mathcal{M}}_i | \phi_k \rangle|^2}. \quad (\text{A4})$$

Combining this result with the limit $0 \leq \langle \beta, \beta | \hat{\mathcal{M}}_i^+ \hat{\mathcal{M}}_i | \beta, \beta \rangle \leq 1$, the upper bound for $Q_{0x}^{M_1}$ and the lower bound for $Q_{0x}^{M_0}$ can be expressed as

$$\begin{aligned} \overline{Q}_{0x}^{M_1} &= \frac{1}{N^+} \left(e^{\frac{\mu}{2}} \sqrt{Q_{\alpha\alpha}^{M_1}} + e^{-\frac{\mu}{2}} \sqrt{Q_{00}^{M_1}} \right)^2 \\ &\quad + \frac{N^-}{N^+} \left(\frac{e^{\mu} N^-}{4} + e^{\mu} \sqrt{Q_{\alpha\alpha}^{M_1}} + \sqrt{Q_{00}^{M_1}} \right), \\ \underline{Q}_{0x}^{M_0} &= \frac{1}{N^+} \left(e^{\frac{\mu}{2}} \sqrt{Q_{\alpha\alpha}^{M_0}} - e^{-\frac{\mu}{2}} \sqrt{Q_{00}^{M_0}} \right)^2 \\ &\quad - \frac{N^-}{N^+} \left(e^{\mu} \sqrt{Q_{\alpha\alpha}^{M_0}} + \sqrt{Q_{00}^{M_0}} \right). \end{aligned} \quad (\text{A5})$$

Here the gains of the state $|\alpha\rangle_{2k-1} |\alpha\rangle_{2k}$ on the monitoring line are $Q_{\alpha\alpha}^{M_0} = (1 - p_d)^3 [1 - (1 - p_d) e^{-2\mu(1-t_B)\eta}] c5$, $Q_{\alpha\alpha}^{M_1} = p_d (1 - p_d)^3 e^{-2\mu(1-t_B)\eta} c5$, where $c5 = (-2e^{-2t_B\mu} + 2e^{-t_B\mu - t_B\mu\eta} + e^{-2t_B\mu\eta})$, and the gains of the states $|0\rangle_{2k-1} |0\rangle_{2k}$ on the monitoring line are $Q_{00}^{M_i} = p_d (1 - p_d)^3$.

Additionally, when Bob applies a active-basis choice measurement setup, the gains $Q_{0z}^{M_i}$, $Q_{1z}^{M_i}$, $Q_{\alpha\alpha}^{M_i}$ and $Q_{00}^{M_i}$ are given by $Q_{0z}^{M_i} = Q_{1z}^{M_i} = c1(1 - c1)$, $Q_{\alpha\alpha}^{M_0} = (1 - p_d) [1 - (1 - p_d) e^{-2\mu(1-t_B)\eta}]$, $Q_{\alpha\alpha}^{M_1} = p_d (1 - p_d) e^{-2\mu(1-t_B)\eta}$ and $Q_{00}^{M_i} = p_d (1 - p_d)$, with other formulas unchanged.

-
- [1] Bennett, C. H. & Brassard, G. Quantum cryptography: public key distribution and coin tossing. In *Proceedings of the Conference on Computers, Systems and Signal Processing*, 175 (IEEE Press, New York, 1984).
 - [2] Ekert, A. K. Quantum cryptography based on bell's theorem. *Phys. Rev. Lett.* **67**, 661–663 (1991).
 - [3] Scarani, V. *et al.* The security of practical quantum key distribution. *Rev. Mod. Phys.* **81**, 1301 (2009).
 - [4] Xu, F., Ma, X., Zhang, Q., Lo, H.-K. & Pan, J.-W. Secure quantum key distribution with realistic devices. *Rev. Mod. Phys.* **92**, 025002 (2020).
 - [5] Pirandola, S. *et al.* Advances in quantum cryptography. *Adv. Opt. Photon.* **12**, 1012–1236 (2020).
 - [6] Lydersen, L. *et al.* Hacking commercial quantum cryptography systems by tailored bright illumination. *Nat. Photonics* **4**, 686–689 (2010).
 - [7] Lo, H.-K., Curty, M. & Qi, B. Measurement-device-independent quantum key distribution. *Phys. Rev. Lett.* **108**, 130503 (2012).
 - [8] Braunstein, S. L. & Pirandola, S. Side-channel-free quantum key distribution. *Phys. Rev. Lett.* **108**, 130502 (2012).
 - [9] Zhou, Y.-H., Yu, Z.-W. & Wang, X.-B. Making the decoy-state measurement-device-independent quantum key distribution practically useful. *Phys. Rev. A* **93**, 042324 (2016).
 - [10] Yin, H.-L. *et al.* Measurement-device-independent quantum key distribution over a 404 km optical fiber. *Phys. Rev. Lett.* **117**, 190501 (2016).
 - [11] Lucamarini, M., Yuan, Z. L., Dynes, J. F. & Shields, A. J. Overcoming the rate–distance limit of quantum key distribution without quantum repeaters. *Nature* **557**, 400–403 (2018).
 - [12] Ma, X., Zeng, P. & Zhou, H. Phase-matching quantum key distribution. *Phys. Rev. X* **8**, 031043 (2018).
 - [13] Wang, X.-B., Yu, Z.-W. & Hu, X.-L. Twin-field quantum key distribution with large misalignment error. *Phys. Rev. A* **98**, 062323 (2018).
 - [14] Lin, J. & Lütkenhaus, N. Simple security analysis of phase-matching measurement-device-independent quantum key distribution. *Phys. Rev. A* **98**, 042332 (2018).
 - [15] Yin, H.-L. & Fu, Y. Measurement-device-independent twin-field quantum key distribution. *Sci. Rep.* **9**, 3045 (2019).
 - [16] Curty, M., Azuma, K. & Lo, H.-K. Simple security proof of twin-field type quantum key distribution protocol. *npj Quantum Inf.* **5**, 64 (2019).
 - [17] Cui, C. *et al.* Twin-field quantum key distribution without phase postselection. *Phys. Rev. Applied* **11**, 034053 (2019).

- [18] Yin, H.-L. & Chen, Z.-B. Coherent-state-based twin-field quantum key distribution. *Sci. Rep.* **9**, 14918 (2019).
- [19] Minder, M. *et al.* Experimental quantum key distribution beyond the repeaterless secret key capacity. *Nat. Photonics* **13**, 334–338 (2019).
- [20] Brassard, G., Lütkenhaus, N., Mor, T. & Sanders, B. C. Limitations on practical quantum cryptography. *Phys. Rev. Lett.* **85**, 1330–1333 (2000).
- [21] Hwang, W.-Y. Quantum key distribution with high loss: Toward global secure communication. *Phys. Rev. Lett.* **91**, 057901 (2003).
- [22] Wang, X.-B. Beating the photon-number-splitting attack in practical quantum cryptography. *Phys. Rev. Lett.* **94**, 230503 (2005).
- [23] Lo, H.-K., Ma, X. & Chen, K. Decoy state quantum key distribution. *Phys. Rev. Lett.* **94**, 230504 (2005).
- [24] Koashi, M. Unconditional security of coherent-state quantum key distribution with a strong phase-reference pulse. *Phys. Rev. Lett.* **93**, 120501 (2004).
- [25] Scarani, V., Acin, A., Ribordy, G. & Gisin, N. Quantum cryptography protocols robust against photon number splitting attacks for weak laser pulse implementations. *Phys. Rev. Lett.* **92**, 057901 (2004).
- [26] Tamaki, K. & Lo, H.-K. Unconditionally secure key distillation from multiphotons. *Phys. Rev. A* **73**, 010302 (2006).
- [27] Yin, H.-L., Fu, Y., Mao, Y. & Chen, Z.-B. Security of quantum key distribution with multiphoton components. *Sci. Rep.* **6**, 29482 (2016).
- [28] Inoue, K., Waks, E. & Yamamoto, Y. Differential phase shift quantum key distribution. *Phys. Rev. Lett.* **89**, 037902 (2002).
- [29] Inoue, K., Waks, E. & Yamamoto, Y. Differential-phase-shift quantum key distribution using coherent light. *Phys. Rev. A* **68**, 022317 (2003).
- [30] Stucki, D., Brunner, N., Gisin, N., Scarani, V. & Zbinden, H. Fast and simple one-way quantum key distribution. *Appl. Phys. Lett.* **87**, 194108 (2005).
- [31] Sasaki, T., Yamamoto, Y. & Koashi, M. Practical quantum key distribution protocol without monitoring signal disturbance. *Nature* **509**, 475–478 (2014).
- [32] Stucki, D. *et al.* Continuous high speed coherent one-way quantum key distribution. *Opt. Express* **17**, 13326–13334 (2009).
- [33] Stucki, D. *et al.* High rate, long-distance quantum key distribution over 250 km of ultra low loss fibres. *New J. Phys.* **11**, 075003 (2009).
- [34] Walenta, N. *et al.* A fast and versatile quantum key distribution system with hardware key distillation and wavelength multiplexing. *New J. Phys.* **16**, 013047 (2014).
- [35] Korzh, B. *et al.* Provably secure and practical quantum key distribution over 307 km of optical fibre. *Nat. Photonics* **9**, 163–168 (2015).
- [36] Sibson, P. *et al.* Chip-based quantum key distribution. *Nat. Commun.* **8**, 2041–1723 (2017).
- [37] Sibson, P. *et al.* Integrated silicon photonics for high-speed quantum key distribution. *Optica* **4**, 172–177 (2017).
- [38] Roberts, G. L. *et al.* Modulator-free coherent-one-way quantum key distribution. *Laser Photonics Rev.* **11**, 1700067 (2017).
- [39] Dai, J., Zhang, L., Fu, X., Zheng, X. & Yang, L. Pass-block architecture for distributed-phase-reference quantum key distribution using silicon photonics. *Opt. Lett.* **45**, 2014–2017 (2020).
- [40] Peev, M. *et al.* *New J. Phys.* **11**, 075001 (2009).
- [41] IDQuantique, Geneva, Switzerland, <https://www.idquantique.com/quantum-sensing/products/clavis>
- [42] Branciard, C., Gisin, N. & Scarani, V. Upper bounds for the security of two distributed-phase reference protocols of quantum cryptography. *New J. Phys.* **10**, 013031 (2008).
- [43] Moroder, T. *et al.* Security of distributed-phase-reference quantum key distribution. *Phys. Rev. Lett.* **109**, 260501 (2012).
- [44] Wang, Y., Primaatmaja, I. W., Lavie, E., Varvitsiotis, A. & Lim, C. C. W. Characterising the correlations of prepare-and-measure quantum networks. *npj Quantum Inf.* **5**, 17 (2019).
- [45] Marco, I. D. *et al.* Real-time operation of a multi-rate, multi-protocol quantum key distribution transmitter. *Optica* **8**, 911–915 (2021).
- [46] González-Payo, J., Trényi, R., Wang, W. & Curty, M. Upper security bounds for coherent-one-way quantum key distribution. *Phys. Rev. Lett.* **125**, 260510 (2020).
- [47] Trényi, R. & Curty, M. Zero-error attack against coherent-one-way quantum key distribution. *arXiv:quant-ph/2101.07192* (2021).
- [48] Beaudry, N. J., Moroder, T. & Lütkenhaus, N. Squashing models for optical measurements in quantum communication. *Phys. Rev. Lett.* **101**, 093601 (2008).
- [49] Cao, Z., Zhou, H., Yuan, X. & Ma, X. Source-independent quantum random number generation. *Phys. Rev. X* **6**, 011020 (2016).
- [50] König, R., Renner, R. & Schaffner, C. The operational meaning of min- and max-entropy. *IEEE Trans. Inf. Theory* **55**, 4337–4347 (2009).
- [51] Renes, J. M. & Renner, R. One-shot classical data compression with quantum side information and the distillation of common randomness or secret keys. *IEEE Trans. Inf. Theory* **58**, 1985–1991 (2012).
- [52] Tomamichel, M. & Renner, R. Uncertainty relation for smooth entropies. *Phys. Rev. Lett.* **106**, 110506 (2011).
- [53] Tomamichel, M., Lim, C. C. W., Gisin, N. & Renner, R. Tight finite-key analysis for quantum cryptography. *Nat. Commun.* **3**, 634 (2012).
- [54] Li, H.-W. *et al.* Attacking a practical quantum-key-distribution system with wavelength-dependent beam-splitter and multiwavelength sources. *Phys. Rev. A* **84**, 062308 (2011).
- [55] Li, H.-W. *et al.* Randomness determines practical security of bb84 quantum key distribution. *Sci. Rep.* **5**, 16200 (2015).
- [56] Sun, S.-H., Tian, Z.-Y., Zhao, M.-S. & Ma, Y. Security evaluation of quantum key distribution with weak basis-choice flaws. *Sci. Rep.* **10**, 18145 (2020).
- [57] Islam, N. T., Lim, C. C. W., Cahall, C., Kim, J. & Gauthier, D. J. Provably secure and high-rate quantum key distribution with time-bin qudits. *Sci. Adv.* **3**, e1701491 (2017).
- [58] Ruska, D., Boaron, A., Curty, M., Martin, A. & Zbinden, H. Security proof for a simplified bennett-brassard 1984 quantum-key-distribution protocol. *Phys. Rev. A* **98**, 052336 (2018).
- [59] Boaron, A. *et al.* Secure quantum key distribution over 421 km of optical fiber. *Phys. Rev. Lett.* **121**, 190502 (2018).

- [60] Boaron, A. *et al.* Simple 2.5 ghz time-bin quantum key distribution. *Appl. Phys. Lett.* **112**, 171108 (2018).
- [61] Liu, H. *et al.* Experimental 4-intensity decoy-state quantum key distribution with asymmetric basis-detector efficiency. *Phys. Rev. A* **100**, 042313 (2019).
- [62] Yin, H.-L. *et al.* Experimental composable security decoy-state quantum key distribution using time-phase encoding. *Opt. Express* **28**, 29479–29485 (2020).
- [63] Chen, Y.-A. *et al.* An integrated space-to-ground quantum communication network over 4,600 kilometres. *Nature* **589**, 214–219 (2021).
- [64] Koashi, M. Simple security proof of quantum key distribution based on complementarity. *New J. Phys.* **11**, 045018 (2009).
- [65] Wang, X.-B., Hu, X.-L. & Yu, Z.-W. Practical long-distance side-channel-free quantum key distribution. *Phys. Rev. Applied* **12**, 054034 (2019).
- [66] Azuma, K. Weighted sums of certain dependent random variables. *Tohoku Math. J.* **19**, 357 – 367 (1967).